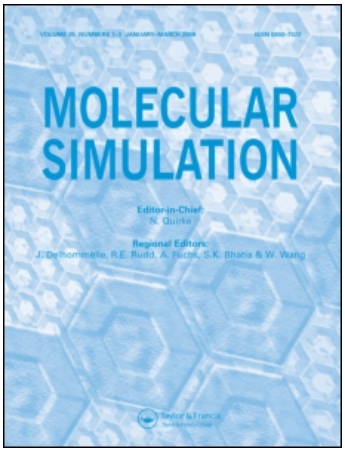

Molecular Simulation
Publication details, including instructions for authors and subscription information:
http://www.informaworld.com/smpp/title~content=t713644482

Molecular Dynamics Simulation of the Liquid-liquid Interface for Immiscible and Partially Miscible Mixtures

Huabing Wang[a]; Eric Carlson[a]; Douglas Henderson[a]; Richard L. Rowley[b]
[a] Department of Chemical Engineering, Brigham Young University, Provo, UT, USA [b] Department of Chemistry, Brigham Young University, Provo, UT, USA

Online publication date: 13 May 2010

To cite this Article Wang, Huabing , Carlson, Eric , Henderson, Douglas and Rowley, Richard L.(2003) 'Molecular Dynamics Simulation of the Liquid-liquid Interface for Immiscible and Partially Miscible Mixtures', Molecular Simulation, 29: 12, 777 — 785
To link to this Article: DOI: 10.1080/0892702031000121842
URL: http://dx.doi.org/10.1080/0892702031000121842

Molecular Simulation, Vol. 29 (12), December 2003, pp. 777–785

Taylor & Francis
Taylor & Francis Group

Molecular Dynamics Simulation of the Liquid–liquid Interface for Immiscible and Partially Miscible Mixtures

HUABING WANG[a], ERIC CARLSON[a], DOUGLAS HENDERSON[b] and RICHARD L. ROWLEY[a,*]

[a]*Department of Chemical Engineering, Brigham Young University, Provo, UT 84602, USA;* [b]*Department of Chemistry, Brigham Young University, Provo, UT, USA*

(Received October 2002; In final form November 2002)

Molecular dynamics (MD) simulations were performed on model interfaces between *n*-hexane and water and between water and 1-hexanol. The SPC/E model was used for water. Organic molecules were modeled with united atom potentials located at heavy nuclei, but included explicit modeling of the alcohol H. The structure of the interface was examined in terms of its position, thickness, roughness, and molecular orientations. Additionally, self diffusion coefficients in each phase and the interfacial tension were determined. Significant differences in the interfacial structure were found between the immiscible and partially miscible systems. The interface for the immiscible system is molecularly sharp with only small dynamic waves or corrugation. On the other hand, the interface in the partially miscible system consists of a molecularly sharp region and a bilayer of hexanol oriented with the OH heads out. Relatively static waves corrugate the inner part of the interface considerably more than that for the immiscible system. Water solubility in the hexanol phase occurs in hydrogen bonded cages formed by the OH groups of the alcohol.

Keywords: Liquid–liquid interface; Model interfaces; Molecular dynamics simulation; Interfacial tension

INTRODUCTION

Processes that occur at the interface between two immiscible or partially miscible liquids are of great interest and technical importance. In biological applications, energy-conversion processes occur at the interface between two liquid phases and many cellular functions are regulated by ion transfer through the liquid–liquid interface (LLI). The design and operation of many processes in the petroleum and chemical industry depend upon accurate knowledge of the structure, interfacial tension and mass transfer characteristics of the LLI, including liquid–liquid extraction, enhanced oil recovery, surfactant technology, etc. Molecular simulation provides an important tool for investigating and modeling the structure and dynamics of the LLI. Molecular simulations can offer new insights, help interpret experimental data and observations, check the accuracy of phenomenological models, and provide quantitative results for process development. Early work used Monte Carlo (MC) [1,2] and molecular dynamics (MD) [3–7] simulations to study the LLI for very simple systems consisting of non-polar atomic solvents or water-membrane structures.

Equilibrium molecular simulations of the LLI have focused on the methodology of simulating the interface, the equilibrium structure (width, corrugation, etc.) of the interface, calculation of the interfacial tension, and its polarizability. An early system studied was the water + *n*-hexane system. Carpenter and Hehre [7] found that the interface for this system was approximately 1 nm in thickness and that significant structuring occurred near the interface. Surprisingly, they concluded that the interface was not molecularly sharp, that some hexane molecules detached from the bulk and were completely surrounded by water. Benjamin [8],

*Corresponding author. E-mail: rowley@byu.edu

ISSN 0892-7022 print/ISSN 1029-0435 online © 2003 Taylor & Francis Ltd
DOI: 10.1080/0892702031000121842

however, in studying the water/1,2-dichloroethane interface found the interface to be molecularly sharp. Thermal fluctuations, however, produced capillaries or fingers into the opposite phase that could be rather long. He also found structural and orientational alignments of the water dipoles that extended two or three molecular layers away from the interface. Molecular orientations, interface structure, interfacial tension, surface roughness, ion solvation, and ion pairing and dissociation have since been studied by molecular simulation for several different systems. For example, the decane/water LLI was studied by van Buuren *et al.* [9], several aqueous/organic LLIs were studied by Michael and Benjamin [10,11], and NaCl in water/1,2-dichloroethane was studied by Schweighofer and Benjamin [12].

Our interest here is in studying a partially miscible system in which the interfacial tension is lower than the traditional oil/water interface because the lower interfacial tension and the mixed nature of the equilibrium phases could significantly alter the interface structure from that previously observed. We report here results of simulations first on a model for the immiscible system water + *n*-hexane and then results on simulations for a model of the partially miscible system water + 1-hexanol. By first studying an oil/water system, we are able to benchmark our methodology and compare our results with those already published, but, more importantly, we establish a reference against which the water + 1-hexanol results can be compared. This latter system is more difficult to simulate and the results are more easily interpreted in terms of differences from the water + *n*-hexane system.

SIMULATIONS

Molecular Models

Throughout this study we use pair-wise additive models to represent the potential energy of the system. Intermolecular pair potentials were taken as the sum of all pair potentials between interaction sites within the molecules. Water was modeled with the SPC/E [13] interaction model, which includes a Lennard–Jones (LJ) potential for oxygen and partial point charges located at the centers of the three nuclei. Organic molecules were modeled with united atom models that treat $-CH_x$ groups as single interacting LJ sites. OPLS parameters were obtained from Ref. [14] for these sites. In the case of 1-hexanol, the hydroxyl hydrogen is treated as a separate site with a point charge but no LJ interactions. Point charges are located on the alpha carbon site in addition to the hydroxyl oxygen and hydrogen nuclei. Bond lengths and angles were rigidly constrained in the simulation at the values obtained from optimization of the isolated molecule using AM1 in Gausian 98 [15], but torsional potentials permitted bond rotations. Values for the parameters used in the models are given in Table I.

Simulation Details

The water + *n*-hexane simulation cell was an elongated box 7.0 nm long (in the *x* direction) with a cross-sectional area of 2.8 nm × 2.8 nm containing 875 water molecules and 125 hexane molecules. For water + 1-hexanol, the simulation cell was further elongated to 9.5 nm with two thirds of the cell occupied by the organic phase. This was done to try

TABLE I Model parameters used in the simulations

Bond distances (nm)								
Water	O–H	0.100						
Hexane	C–C	0.154						
Hexanol	C–C	0.154	C–O	0.144	O–H	0.099		
Bond angles (degrees)								
Water	HOH	109						
Hexane	CCC	112						
Hexanol	CCC	112	CCO	113	COH	104		
Partial charges (e)								
Water	O	− 0.848	H	0.424				
Hexane	C	0						
Hexanol	α–C	0.265	all other C	0	O	− 0.700	H	0.435
LJ ε/k parameters (K)								
Water	O	78.2	H	0				
Hexane	CH_3	88.1	CH_2	59.4				
Hexanol	CH_3	88.1	CH_2	59.4	O	85.56	H	0
LJ σ parameters (nm)								
Water	O	0.317	H	0				
Hexane	CH_3	0.391	CH_2	0.391				
Hexanol	CH_3	0.391	CH_2	0.391	O	0.307	H	0

and maximize the extent of the phase into which interfacial structuring predominantly extends. Twelve hundred molecules were used in this simulation, 244 hexanol and 956 water molecules. The initial cross sectional area of the simulation box was adjusted to its final value during the equilibration in order to achieve the appropriate liquid density. NVT simulations were used following this adjustment. All simulations reported in this work correspond to 298.15 K. With a time step size of 2.5 fs, 50,000 time steps were required to equilibrate the hexane simulations and 100,000 time steps were required to equilibrate the hexanol simulations due to the larger degree of structure of the interface. A fourth-order-correct predictor-corrector method was used to integrate the equations of motion, and the particle–particle/particle mesh (PPPM) [16,17] technique was used to treat the long-range Coulombic interactions.

In the case of water + *n*-hexane, simulations were initiated by placing water molecules at random positions in the left side of the simulation cell and hexane molecules in the right side. Additional simulations were performed with two initially homogeneous mixed phases, and separation of the components was observed during the equilibration process. After equilibration, the two components were found to be insoluble, within the resolution of our cell size, independent of the starting configuration. This was not true for the water + 1-hexanol system. For this system, our model showed little solubility of 1-hexanol in the water phase in agreement with experiment. However, the solubility limit for water in the organic phase could not be discerned from the simulation itself. When starting from mixed initial conditions, the 1-hexanol molecules rather quickly left the aqueous phase, but the water molecules in the organic phase remained trapped for the duration of our simulation capability. This is true up to compositions of 45 mol%, even though the experimental solubility is 30 mol%. As we discuss later, this is because the water dissolves in molecular-sized micelles that grow as water is added to the phase, and there is no way to distinguish in our simulation between stable and metastable (super-saturated) solubility states. Instead, we performed independent osmotic molecular dynamics (OMD) simulations [18] to determine the equilibrium solubility for the molecular models used here. Activity coefficients obtained from the OMD simulations produced solubility limits of 93 and 35 mol% water in the two phases. The uncertainties for these numbers, however, are rather large and we never saw any *n*-hexanol dissolve in the bulk aqueous phase. All of the results described here for the LLI were performed with 30 mol% water in 1-hexanol.

Interfacial Property Calculations

The interfacial tension was determined from the difference between the tranverse (y and z) and perpendicular (x) components of the pressure tensor. The pressure tensor components, $P_{\alpha\beta}$, were calculated from the positions, r, and velocities, v, of the molecules using the virial equation

$$P_{\alpha\beta} = \frac{1}{V}\left(\sum_{i=1}^{N} m_i v_{i_\alpha} v_{i_\beta} + \sum_{i=1}^{N-1}\sum_{j=i+1}^{N} F_{ij_\alpha} r_{ij_\beta}\right), \quad (1)$$

where the subscript i refers to molecule i and ij refers to the force, F, or distance between the i and j molecular centers. The surface tension was then calculated from the diagonal terms of the pressure tensor using

$$\gamma = -\frac{L}{2}\left(\frac{P_{yy} + P_{zz}}{2} - P_{xx}\right). \quad (2)$$

where L is the formal box length in the x direction. As has been done by others [10], the cross sectional area of the simulation cell was divided into a $N \times N$ array of sub boxes that run the length of the actual cell, illustrated in Fig. 1. This permits a finer resolution of the molecular nature of the interface as local interface position and width can be found in each of the N^2 sub cells. Our definition of the interfacial location within each sub cell, h_{ij}, is the same as that previously used [10], namely,

$$h_{ij} = \frac{1}{2}\left[(\max x)_{ij_{\text{water}}} + (\min x)_{ij_{\text{organic}}}\right]. \quad (3)$$

It is therefore the average of the maximum x location for any water oxygen site contained within the ij sub cell and the minimum x location of any site on an organic molecule contained within the same sub cell. The local surface positions are then used to generate a histogram from which the probability distribution of the interface can be observed. Sub cell interface positions provide a measure of the roughness of the surface and the width of the location histogram is a measure of the dynamic nature of this roughness.

The local interface width was also calculated in each of the N^2 sub cells using a modified version of that previously used [10],

$$w_{ij} = (\max x)_{ij_{\text{water}}} - (\min x)_{ij_{\text{organic}}} + \frac{\sigma_{\text{water}} + \sigma_{\text{organic}}}{2}, \quad (4)$$

where σ is the LJ size parameter of the two sites involved, the oxygen site of the water molecule and the site on the organic molecule with the minimum x value, respectively. The addition of the last term in Eq. (4) references the width to the size of the interacting species and eliminates negative widths. For example, a theoretical perfectly-aligned interface

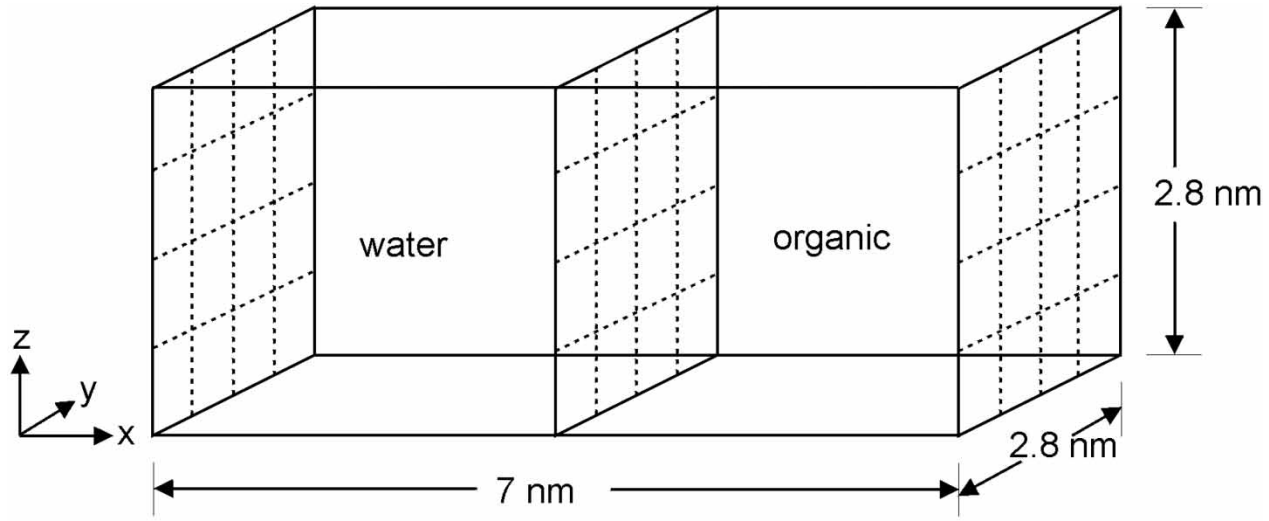

FIGURE 1 Simulation cell showing geometry, dimensions in nm, and division of the simulation volume into $N \times N$ ($N = 4$ is depicted by the dashed lines) sub cells.

of hard spheres of the same diameter arranged such that the spheres on opposite sides of the interface just touch would have zero interfacial width by Eq. (4), but a negative value if the last term is not included. The width is a measure of the sharpness of the interface and its distribution reflects the dynamic stability of its sharpness.

RESULTS

Water + *n*-Hexane

In contrast to the results obtained by Carpenter and Hehre [7] for this system, we found the interface to be molecularly sharp, stable, and consistent with the experimental insolubility of hexane and water. Our observations are consistent with those of Buuren *et al.* [9] for the decane + water interface.

The density histogram shown in Fig. 2 shows that the two bulk fluids are separated by a rather sharp interface. There appears to be little orientation of the hexane molecules in the organic phase as there is no distinction between the histograms for the various carbon sites. This was also confirmed by examining the distribution of an end-to-end vector between the two sites representing $-CH_3$ centers. The end-to-end vectors were randomly oriented in the bulk but were strongly oriented very near the interface at 90° to an interface-normal vector. Similarly, the water dipole vector in the interfacial region is strongly oriented at 90° to the interface normal as shown in Fig. 3.

The average interface location is seen in Fig. 4a to be at the center of the 7.0 nm cell. The location is independent of the number of sub cells used in producing the histogram indicating a molecularly smooth interface without large protrusions or

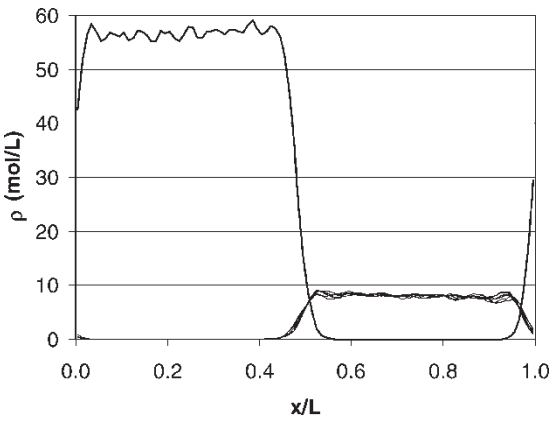

FIGURE 2 Density profiles of LJ sites for O (single line, left) and C (one line for each C site, right).

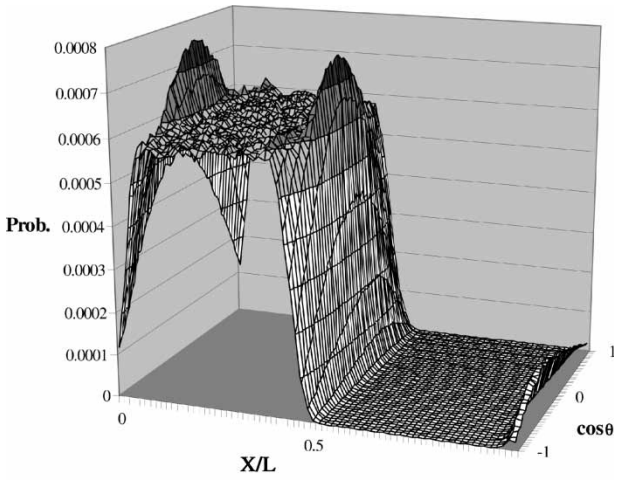

FIGURE 3 Water dipole vector orientation as a function of cell position where θ represents the angle between a vector normal to the interface and the dipole vector.

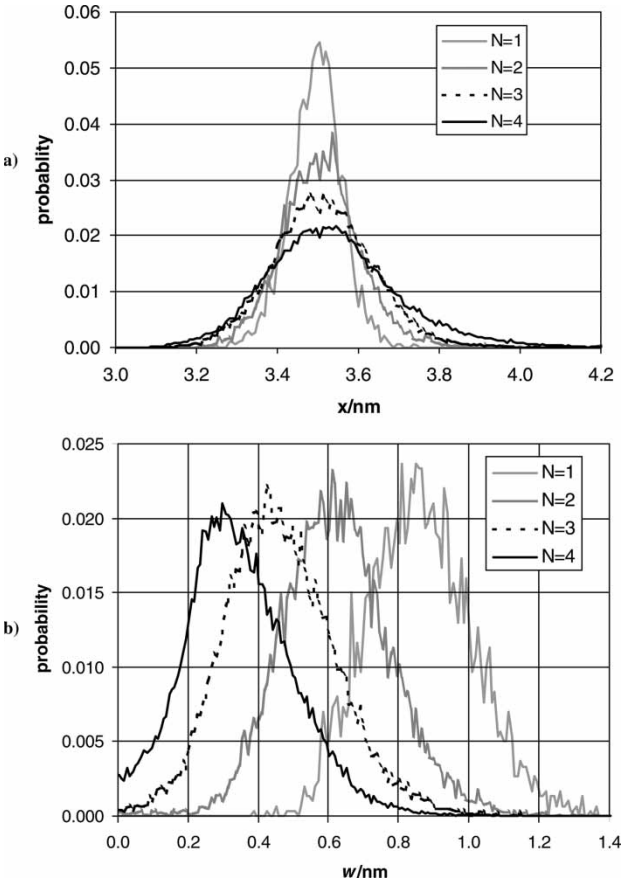

FIGURE 4 Interface location (a) and width (b) in nm for the water + *n*-hexane system as a function of *N*.

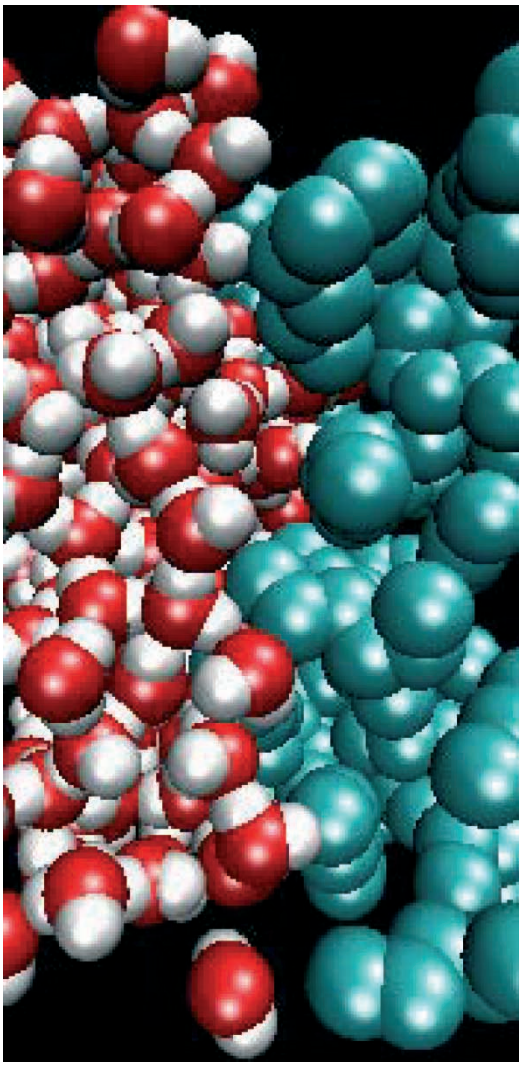

FIGURE 5 Snapshot of the simulated interfacial region illustrating interfacial structure.

fingers. The breadth of the location histogram increases with larger *N* indicating that there is some corrugation to the interface or small waves. The asymmetry of the histograms suggests that these waves penetrate into the organic phase whereas the water side of the interface is less susceptible to movement.

The interface width, shown in Fig. 4b, shows considerable dependence upon the number of sub cells used to compute the histogram. This is also indicative of the surface roughness since the larger the surface area used to calculate the interfacial width, the larger the width. While the peak in the interfacial width distribution shifts with *N*, the breadth of the distribution appears to be independent of *N*, suggesting a dynamic nature to the roughness; i.e., that the waves are not standing waves in a particular location. Figure 5 is a snapshot of the interfacial region within the cell that illustrates the molecular nature of the interfacial roughness.

The interfacial tension calculated for this model interface is 56 ± 6 dyn/cm at 298.15 K. This may be compared to the experimental value of 51 dyn/cm. Values obtained for the interfacial tension from Eq. (2) were quite noisy and were therefore time averaged for 1.36×10^7 steps, or 34 ns. The precision reported is based on eight block averages of 1.7×10^6 steps each. An interfacial resistance to mass transfer would be characteristic of a system with a large interfacial tension such as that observed here. This interfacial resistance is observed in the decline of the self diffusion coefficients near the interface. These trends are shown in Fig. 6 where the calculated self diffusion coefficients in each phase decline near the interface, both for the transverse and perpendicular directions relative to the interface. Note that transverse values are larger throughout the simulation cell, but mobility in both directions decrease in the interfacial region.

As might be expected, the interfacial tension and the structure of the interface are coupled to the breaking of the hydrogen bond structure. We find an average of 4.5 hydrogen bonds per water molecule in the bulk structure, but that number begins to decline within 0.2 nm of the interface and decreases to about

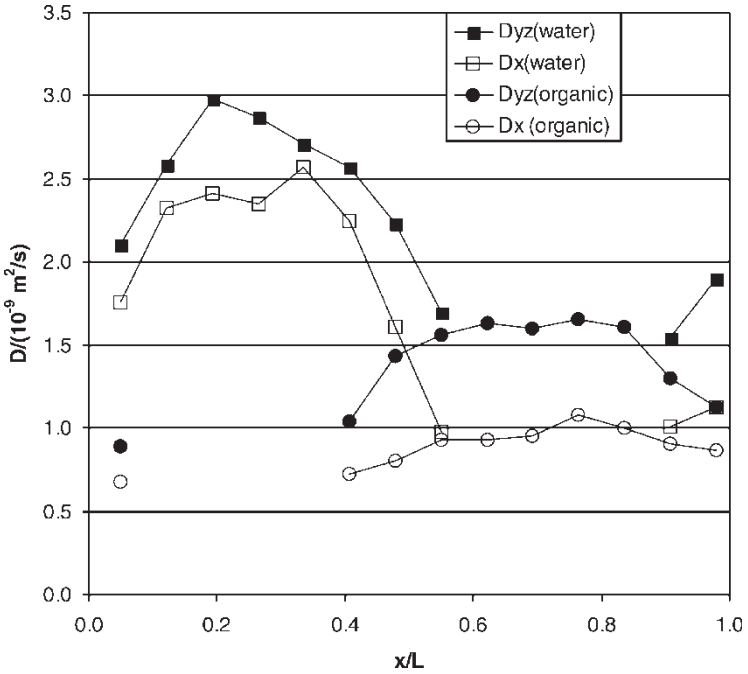

FIGURE 6 Self diffusion coefficients for water (squares) and *n*-hexane (circles) in the transverse (filled symbols) and *x* (open symbols) directions.

2.8 hydrogen bonds per water molecule at the center of the interface.

Water + 1-Hexanol

The structure of the interface in the partially miscible water + 1-hexanol system is significantly different from that of water + *n*-hexane. Figure 7 illustrates the remarkable interface structure that extends at length into the organic phase. Note that the 1-hexanol molecules are highly ordered near the contact between the water and hexanol molecules into a bilayer that must be considered part of the interface. At the inner part of the interface where water first contacts the alcohol, the alcohol OH heads penetrate into the interface and the carbon chain is oriented perpendicular to the interface. These distinct peaks for the carbon sites, ordered from the interface outward in the same order as they appear in the molecule from head to tail, indicate a high degree of alignment in the *x* direction. Note also the larger $-CH_3$ peak and the inverse order in the next set of ordered peaks. This depicts a structure in which the 1-hexanol molecules form a double layer, tail to tail, that excludes water from this portion of the interfacial region. The collection of OH heads to the right of this bilayer form hydrogen bonding regions, which solubilize the water. These molecular-scale

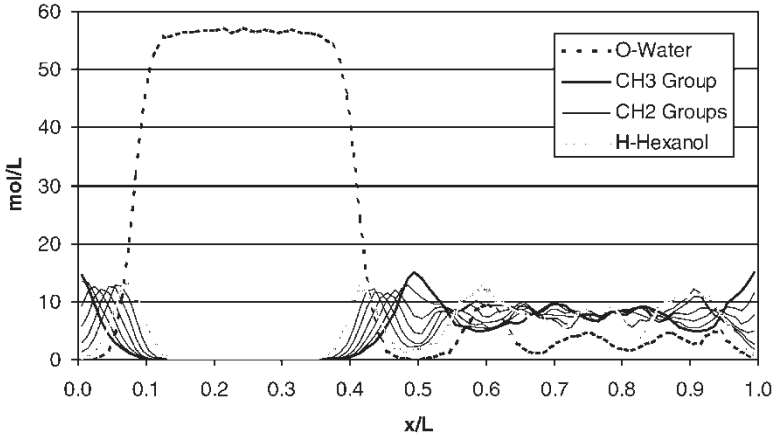

FIGURE 7 Density histogram for water + 1-hexanol simulation for the interaction sites: (– – –) O–water, (————) CH_3–hexanol, (————) all CH_2–hexanol, (▬▬▬) H–hexanol. At the interface, the CH_3 peaks (all same line type) are in the same order, from bulk water to bulk organic phase, as the sites appear in the molecule from –OH group down the chain to the $-CH_3$ group.

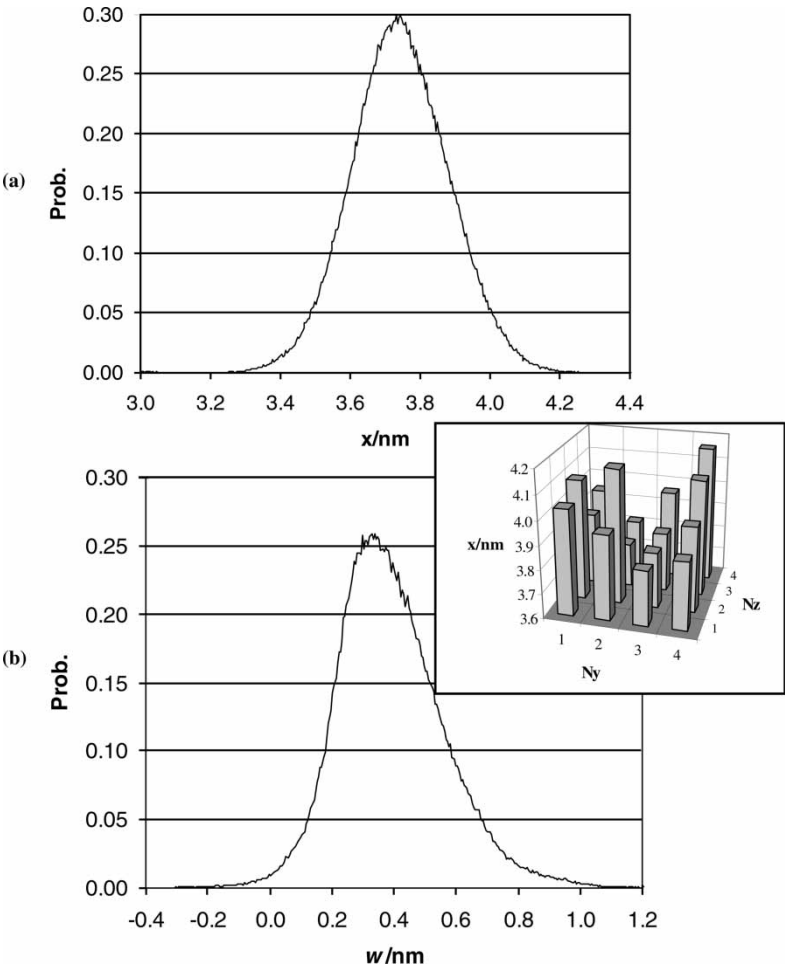

FIGURE 8 Interface position (a) and width (b) for the water + 1-hexanol system for $N = 4$. Inset shows histogram of position as calculated from time averages of the 16 sub cells independently.

micelles appear to be the structural basis of the large solubility of water in hexanol. It is also the reason that we are unable to identify the exact solubility limit of our model system. As additional water is added in the hexanol phase, these hydrogen-bonded micellar regions can grow in size. With no gravitational field in our simulation, we have no way of distinguishing between stable soluble states and metastable super-saturated states. These OH-dominated regions within the hexanol phase that stabilize water solubility are formed by the alcohol, not the water. This was determined by comparing two density profile plots, one for the system with 30 mol% water in the organic phase and one with no water in the organic phase. The density plots were virtually identical for the two systems. Even with no water in the hexanol phase, the density profile shows the bilayer structure in the interfacial region with a strong subsequent OH peak indicating that the OH cages formed by the alcohol hydrogen bonds are present even with no dissolved water.

The interface location information for $N = 4$ shown in Fig. 8a shows a slightly broader peak than was the case for the immiscible system with an asymmetry that indicates a tendency for larger waves or fingers into the organic phase. We have also averaged the interface location separately for the sub cells in the case of $N = 4$. This is shown as an inset in Fig. 8. Note the large amplitude wave indicated by this average. It should be remembered that these are time-averaged data, and so the wavy surface shown in this inset is a persistent wave of large inertia, it is not particularly dynamic during the length of our simulations. Although the interface for the partially miscible system is significantly wider than the immiscible system due to the organic bilayer structure that is approximately 0.2 nm wide, the width for just the inner contact region as calculated from Eq. (4) (comparing the $N = 4$ value in each case) is 0.3 nm, as shown in Fig. 8b, just as it was for the immiscible system. This contact region is molecularly sharp at the local level described by the $N = 4$ sub cells. However, due to the large waves the contact region for $N = 1$ is obviously much larger.

These significant features of the water–1-hexanol interface are perhaps more easily viewed in Fig. 9,

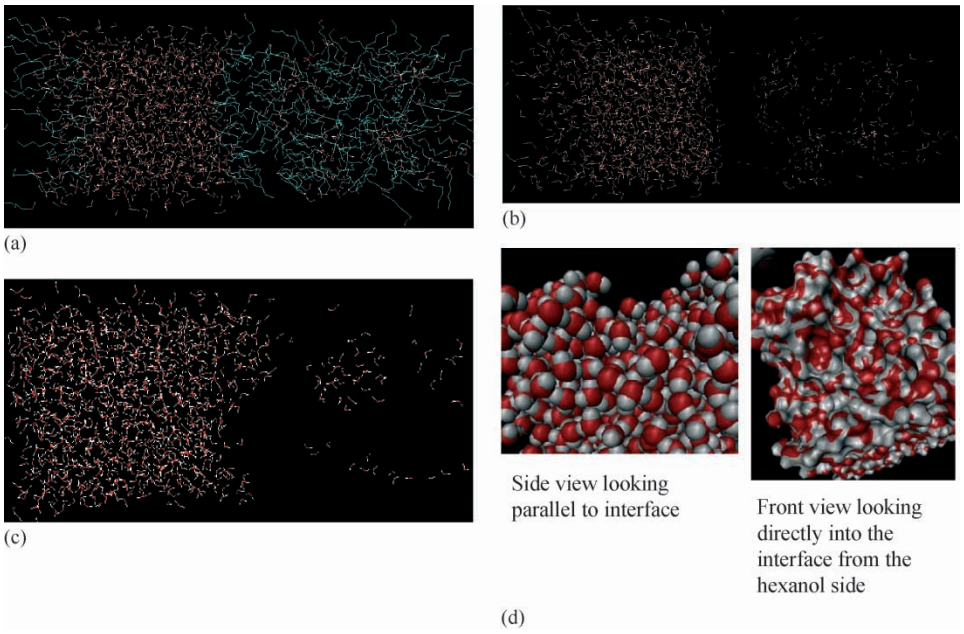

FIGURE 9 Snapshots of the water + hexanol interface: (a) interfacial bilayer, (b) no carbon sites displayed, (c) wave nature of molecular portion of interface, (d) side and direct frontal views of interface.

which illustrates through snapshots the features previously identified. Note in Fig. 9a the presence of the structured hexanol bilayer followed by a region of high OH density that captures the solubilized water. The hexanol molecules have been removed in Fig. 9b to illustrate the regions of high OH and H_2O density in the two-component mixture on the right. The roughness of the contact portion of the interface, though molecularly sharp, is seen to be caused by large waves of water in Fig. 9c. Figure 9d illustrates that roughness with a side and front view of the interface.

The interfacial tension for this system was also calculated from Eqs. (1) and (2). The calculated value for the simulation was 0 ± 1 dyn/cm which can be compared to the experimental value of 7 dyn/cm at 298.15 K. The large waves at the contact interface are consistent with the small interfacial tension calculated here, although we were somewhat surprised that the organic bilayer does not raise the interfacial tension above the value calculated. We suspect that this is because water can form hydrogen bonds on either end of the bilayer equally well, a fact consistent with the observation that water molecules seldom move from the hydrogen-bonded cages in the organic phase into the water phase. We plan in future work to observe the transport of ions through the interface and to probe the interfacial resistance to mass transfer. The relatively linear alignment of the carbon backbones of the hexanol molecules observed in this work is expected to be an important factor in mass transfer through the interface.

CONCLUSIONS

We have performed MD simulations on models for the immiscible water + *n*-hexane and the partially miscible water + 1-hexanol systems. There are significant differences between the structures of the two types of systems. The interface for the immiscible system is molecularly sharp with only small dynamic waves or corrugation. On the other hand, the interface in the partially miscible system consists of a molecularly sharp region and a bilayer of hexanol oriented with the OH heads out. The inner part of the interface where contacts between the water and OH heads occur is highly corrugated or rough with relatively static waves. On this very rough interfacial surface is layered the hexanol bilayer.

The models accurately reproduce several properties including solubility, diffusion coefficients and surface tension. Additionally, the simulations of the partially miscible system provide valuable structural information about the nature and structure of the relatively large solubility of water in hexanol and the low solubility of hexanol in water.

Acknowledgements

Financial support of this work by the American Chemical Society through a type AC Petroleum Research Fund grant and by Brigham Young University through an Undergraduate Mentoring Environment grant is gratefully acknowledged.

References

[1] Linse, P. (1987) "Monte Carlo simulation of liquid–liquid benzene–water interface", *J. Chem. Phys.* **86**, 4177.

[2] Gao, J. and Jorgensen, W.L. (1988) "Theoretical examination of hexanol–water interfaces", *J. Phys. Chem.* **92**, 5813.

[3] Hayoun, M., Meyer, M., Mareschal, M., Ciccotti, G. and Turq, P. (1987) "Molecular dynamics simulation of a liquid–liquid interface", In: Moreau, M. and Turq, P., eds, *Chemical Reactivity in Liquids* (Plenum, New York).

[4] Meyer, M., Mareschal, M. and Hayoun, M. (1988) "Computer modeling of a liquid–liquid interface", *J. Chem. Phys.* **89**, 1067.

[5] Smit, B. (1988) "Molecular dynamics simulations of amphiphilic molecules at a liquid–liquid interface", *Phys. Rev. A* **37**, 3431.

[6] Smit, B., Hilbers, P.A.J., Esselink, K., Rupert, L.A.M., van Os, N.M. and Schlijper, A.G. (1991) "Structure of a water oil interface in the presence of micelles: a computer simulations study", *J. Phys. Chem.* **95**, 6361.

[7] Carpenter, I.L. and Hehre, W.J. (1990) "A molecular dynamics study of the hexane water interface", *J. Phys. Chem.* **94**, 531.

[8] Benjamin, I. (1992) "Theoretical study of the water/1,2-dichloroethane interface: structure, dynamics, conformational equilibria at the liquid–liquid interface", *J. Chem. Phys.* **97**, 1432.

[9] van Buuren, A.R., Marrink, S.-J. and Berendsen, H.J.C. (1993) "A molecular dynamics study of the decane/water interface", *J. Phys. Chem.* **97**, 9206.

[10] Michael, D. and Benjamin, I. (1995) "Solute orientational dynamics and surface roughness of water/hydrocarbon interfaces", *J. Phys. Chem.* **99**, 1530.

[11] Michael, D. and Benjamin, I. (2001) "Molecular dynamics computer simulations of solvation dynamics at liquid/liquid interfaces", *J. Chem. Phys.* **114**, 2817.

[12] Schweighofer, K. and Benjamin, I. (2000) "Ion pairing and dissociation at liquid/liquid interfaces: molecular dynamics and continuum models", *J. Chem. Phys.* **112**, 1474.

[13] Berendsen, H.J.C., Grigera, J.R. and Straatsma, T.P. (1987) "The missing term in effective pair potentials", *J. Chem. Phys.* **91**, 6269.

[14] Jorgensen, W.L. (1981) "Quantum and statistical mechanical studies of liquids. 10. Transferable intermolecular potential functions for water, alcohols, ethers. Application to liquid water", *J. Am. Chem. Soc.* **103**, 335.

[15] Frisch, M.J., Trucks, G.W., Schleget, H.B., *et al.* (1998) *Gaussian 98, Revision A.6* (Gaussian, Pittsburgh, PA).

[16] Hockney, R.W. and Eastwood, J.W. (1988) *Computer Simulation Using Particles* (Institute of Physics, Bristol).

[17] Crozier, P.S. and Rowley, R.L. (2000) "Molecular dynamics calculations of the electrochemical properties of electrolyte systems between charged electrodes", *J. Chem. Phys.* **113**, 9202.

[18] Crozier, P.S. and Rowley, R.L. (2002) "Activity coefficient prediction by osmotic molecular dynamics", *Fluid Phase Equilibr.* **193**, 53.